

# Fatigue Behaviors of Ultra Fine Wires of -Type and -Type Titanium Alloys

著者	Satoshi Yonezawa, Takayuki Narushima, Kyosuke Ueda, Hisamichi Kimura, Chiaki Ouchi, Yasutaka Iguchi
journal or publication title	Materials Transactions
volume	50
number	7
page range	1713-1719
year	2009-07-01
URL	<a href="http://hdl.handle.net/10097/00127757">http://hdl.handle.net/10097/00127757</a>

doi: 10.2320/matertrans.MF200920

# Fatigue Behaviors of Ultra Fine Wires of $\beta$ -Type and $\alpha$ -Type Titanium Alloys

Satoshi Yonezawa<sup>1,\*1</sup>, Takayuki Narushima<sup>1</sup>, Kyosuke Ueda<sup>1</sup>,  
Hisamichi Kimura<sup>2</sup>, Chiaki Ouchi<sup>1</sup> and Yasutaka Iguchi<sup>1,\*2</sup>

<sup>1</sup>Department of Materials Processing, Tohoku University, Sendai 980-8579, Japan

<sup>2</sup>Institute for Materials Research, Tohoku University, Sendai 980-8577, Japan

Fatigue behaviors of ultra fine wires of  $\beta$ -type Ti-14Mo-3Nb-1.5Zr alloy and  $\alpha$ -type Ti-10Zr alloy and  $\alpha$ -type CP (commercially pure) titanium with diameters in the range of 35–100  $\mu\text{m}$  were investigated by rotating-bending fatigue testing in 1 mass% lactic acid solution maintained at 310 K. The maximum number of cycles during fatigue testing was  $10^7$ . The  $\beta$ -type Ti-14Mo-3Nb-1.5Zr alloy wires showed a clear fatigue limit. On the other hand, the  $\alpha$ -type Ti-10Zr alloy wire and  $\alpha$ -type CP titanium wire did not show a clear fatigue limit, and their fatigue strengths gradually decreased with decreasing maximum bending stress. The fatigue limit of a  $\beta$ -type Ti-14Mo-3Nb-1.5Zr alloy wire with a polished surface was greater than 50% of its tensile strength, while the fatigue limits of titanium wires with as-drawn surfaces were less than 50% of their tensile strengths. Surface defects that were introduced during the cold drawing process of the wires might act as crack origins of the fatigue fracture. Therefore, surface polishing is an effective technique for improving fatigue properties of titanium wires. The elution of metallic ions from the wires into the 1 mass% lactic acid solution was suppressed at a very low level during fatigue testing of all the investigated titanium wires. [doi:10.2320/matertrans.MF200920]

(Received January 26, 2009; Accepted February 23, 2009; Published April 8, 2009)

**Keywords:** titanium wire, lactic acid solution, elution, fatigue limit, rotating-bending fatigue testing

## 1. Introduction

Functional electrical stimulation (FES) is the controlled application of an electric field near a motor nerve to achieve external control over a motor unit.<sup>1)</sup> The electrode of an FES system is the interface that transmits programmed electrical signals to the neuromuscular systems of the extremities.<sup>2)</sup> The present authors have developed a percutaneous intramuscular electrode for the FES system.<sup>2,3)</sup> The electrode is made from a helically coiled rope wound from 19 strands of hard drawn wires of austenitic stainless steel. The diameter of each wire is 25  $\mu\text{m}$ . However, in the percutaneous FES system, daily maintenance of the region around the lead exit sites is required in order to avoid infection; this is burdensome to patients and their families. Therefore, it is desirable for an FES system to be totally implantable.<sup>4)</sup> The functional requirements of an electrode of a totally implantable FES system are that it should be more biocompatible and reliable than an electrode of a percutaneous FES system, because its replacement is not easy and it is expected to function for at least ten years after implantation.

Titanium and its alloys have been widely employed in dental and medical implants because of their excellent properties such as low density, high corrosion resistance, excellent strength-ductility balance and biocompatibility.<sup>5)</sup> Therefore, titanium can potentially be used as a source material for the electrode of a totally implantable FES system. Fatigue properties of fine-diameter wires made of titanium materials under biological conditions should be elucidated in order to use them in an FES electrode. Although the fatigue properties of fine-diameter titanium wires are essential data for clinical applications, they have not yet been investigated. Recently, our group developed a new  $\beta$ -type

titanium alloy, Ti-14 mass%Mo-3 mass%Nb-1.5 mass%Zr (hereafter referred to as Ti-14Mo-3Nb-1.5Zr), which has excellent cold workability and biocompatibility<sup>6)</sup> for manufacturing cold-drawn titanium wires with diameters of less than 50  $\mu\text{m}$ .

In this study, fatigue behaviors of cold-drawn titanium wires made of the  $\beta$ -type Ti-14Mo-3Nb-1.5Zr alloy,  $\alpha$ -type Ti-10 mass%Zr (hereafter referred to as Ti-10Zr) alloy and  $\alpha$ -type commercially pure titanium (hereafter referred to as CP titanium) with diameters in the range of 35–100  $\mu\text{m}$  were investigated by rotating-bending fatigue testing in 1 mass% lactic acid solution maintained at 310 K. In a previous study, experimental techniques for investigating the fatigue properties of stainless steel wires were established.<sup>3)</sup> In the present study, fatigue strength and elution of ions into the solution during fatigue testing were measured, and fracture surfaces of the wires were observed.

## 2. Experimental

$\beta$ -type Ti-14Mo-3Nb-1.5Zr titanium wires (Hiyama Rare-Metal Industry, Koga, Japan),  $\alpha$ -type Ti-10Zr alloy wire (Hiyama Rare-Metal Industry, Koga, Japan) and  $\alpha$ -type CP titanium wire (Nilaco, Tokyo, Japan) were used as specimens for fatigue testing. These wires were fabricated by a cold drawing process. The diameters and tensile strengths of the specimen wires are summarized in Table 1. Side views and cross sections of the specimen wires are shown in Fig. 1. The Ti-14Mo-3Nb-1.5Zr alloy wire with a diameter of 89  $\mu\text{m}$  has a polished surface, while the other two Ti-14Mo-3Nb-1.5Zr alloy wires with diameters of 35 and 100  $\mu\text{m}$  have as-drawn surfaces. The tensile strengths listed in Table 1 were measured using a mechanical strength testing machine (Instron4301).

The fatigue strength of the wires was measured using a dual-axle-driven rotating-bending fatigue machine.<sup>3)</sup> A pair of axles was rotated in opposite directions, which led to

\*1Graduate Student, Tohoku University

\*2Present address: Hachinohe National College of Technology, Hachinohe 039-1192, Japan

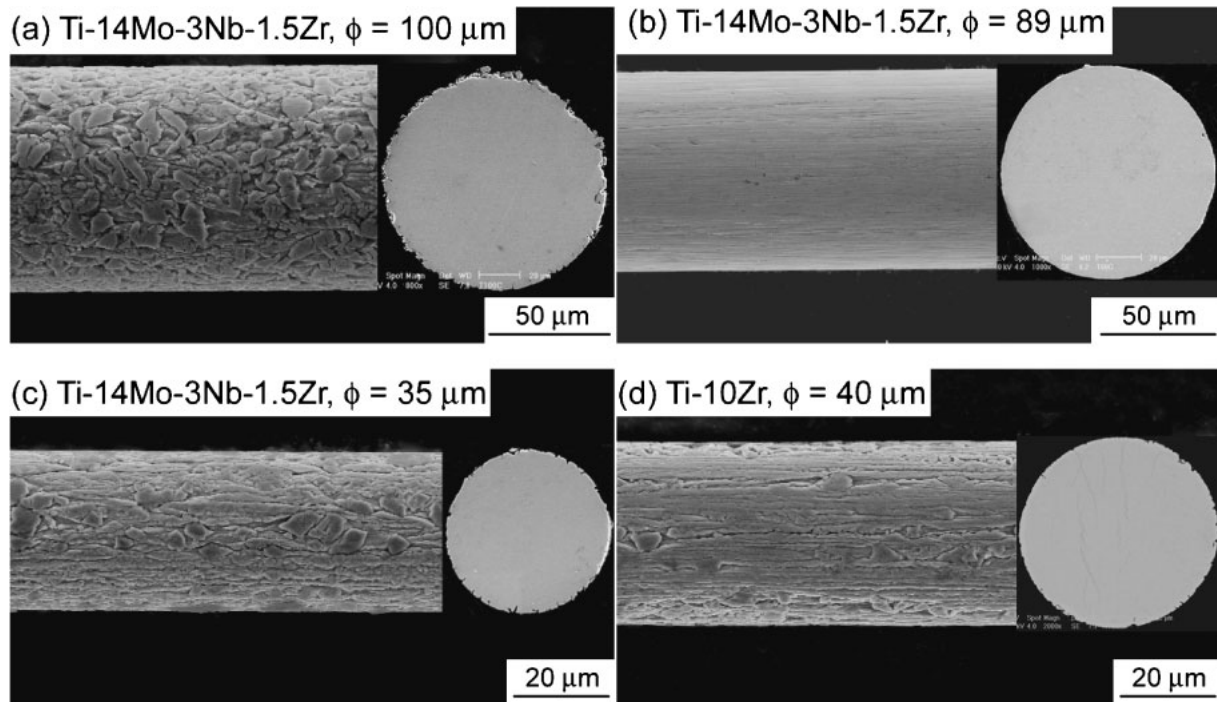


Fig. 1 SEM images of side views and cross sections of titanium alloy wires before fatigue testing in 1 mass% lactic acid solution.

Table 1 Titanium wires used in this study.

Type	Materials	Diameter, $\phi$ ( $\mu\text{m}$ )	Tensile Strength, $\sigma_U$ (MPa)	Surface
$\beta$	Ti-14Mo-3Nb-1.5Zr	100	1224	as-drawn
$\beta$	Ti-14Mo-3Nb-1.5Zr	89	1176	polished
$\beta$	Ti-14Mo-3Nb-1.5Zr	35	1309	as-drawn
$\alpha$	Ti-10Zr	40	1296	as-drawn
$\alpha$	CP-Ti	50	880	as-drawn

repeated bending of the specimen wire. The rotation rate of the axles was fixed to 1000 rpm. The bending stress was varied by changing the distance between the two axles from 4 mm to 30 mm. The maximum bending stress ( $\sigma$ ) was roughly estimated using the following equation:<sup>7)</sup>

$$\sigma = E\phi/D \quad (1)$$

where  $E$  is the Young's modulus of titanium materials,  $\phi$  is the diameter of the specimen wire and  $D$  is the diameter of the curved part of the specimen wire. Values of 110 GPa<sup>8)</sup> and 90 GPa<sup>6)</sup> were used as the Young's moduli of the  $\alpha$ - and  $\beta$ -type titanium materials, respectively. Fatigue testing was stopped when the specimen wire failed or the number of cycles reached  $10^7$ . During fatigue testing, the curved part of each specimen wire was immersed in 1 mass% lactic acid solution maintained at 310 K with an initial pH of 2.2.<sup>3)</sup> The solution volume was 35 cm<sup>3</sup>. After fatigue testing, the fracture surfaces and side surfaces of the wires were observed using a scanning electron microscope (SEM, XL30-FEG, Philips). The solution after fatigue testing was filtered using a membrane filter made of polycarbonate; the pore size of the filter was 0.2  $\mu\text{m}$ . The metallic ion concentration of the filtrate was quantitatively determined by inductively coupled plasma-atomic emission spectroscopy (ICP-AES, ICPS8100,

Shimadzu). The concentration of metallic ions eluted from the titanium wires was compared with that obtained by a static immersion test. In the static immersion test, a titanium wire with a length of 30 mm was statically immersed in 1 mass% lactic acid solution (35 cm<sup>3</sup>) maintained at 310 K for 600 ks, which corresponded to a fatigue testing time of  $10^7$  cycles.

Hardness distributions of cross sections of the titanium wires were measured using a micro-Vickers hardness tester (HM-102, Akashi) with a load of 10 gf.

### 3. Results and Discussion

#### 3.1 Fatigue limit

Fatigue curves of Ti-14Mo-3Nb-1.5Zr alloy wires with diameters of 100  $\mu\text{m}$ , 89  $\mu\text{m}$  and 35  $\mu\text{m}$  obtained during rotating-bending fatigue testing in 1 mass% lactic acid solution are shown in Fig. 2. The arrowheads in the figure indicate that the specimen wire did not fail up to  $10^7$  cycles. For the Ti-14Mo-3Nb-1.5Zr alloy wires with diameters of 100  $\mu\text{m}$ , 89  $\mu\text{m}$  and 35  $\mu\text{m}$  at maximum bending stresses of 303 MPa, 668 MPa and 525 MPa, respectively, failure was not observed up to  $10^7$  cycles. Therefore, the fatigue limits of these wires can be evaluated to be in the ranges of 303–364 MPa, 668–801 MPa and 525–630 MPa, respectively.

Figures 3(a)–(i) show fracture surfaces of the Ti-14Mo-3Nb-1.5Zr alloy wires after fatigue testing. Each fracture surface consists of two regions, the fatigue crack propagation region and the final overload region.<sup>9)</sup> However, in the wire with the diameter of 35  $\mu\text{m}$ , these two regions cannot be observed as clearly as those in the other two wires with larger diameters. Crack origins are observed at edges of the fracture surfaces. Generally, the alternating load forms a slip band on the metallic surface, which develops with increasing number of cycles and acts as the fatigue crack. As shown in Fig. 1,

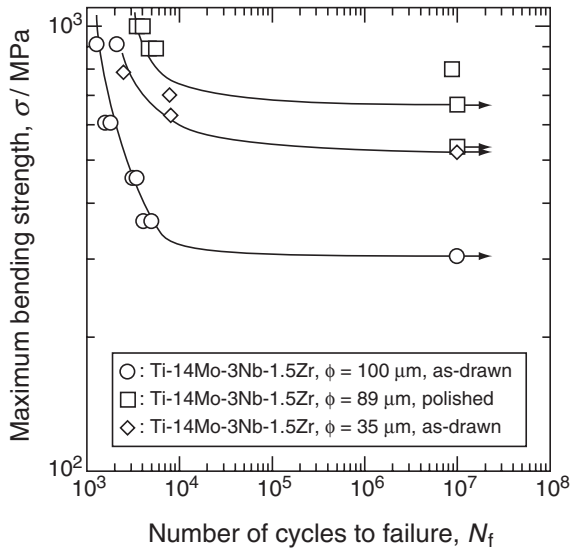


Fig. 2 Fatigue curves of  $\beta$ -type alloy wires in rotating-bending fatigue testing in 1 mass% lactic acid solution.

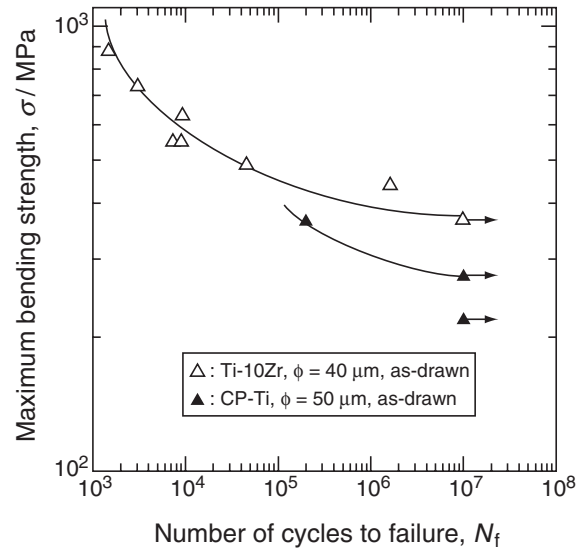


Fig. 4 Fatigue curves of  $\alpha$ -type titanium wires in rotating-bending fatigue testing in 1 mass% lactic acid solution.

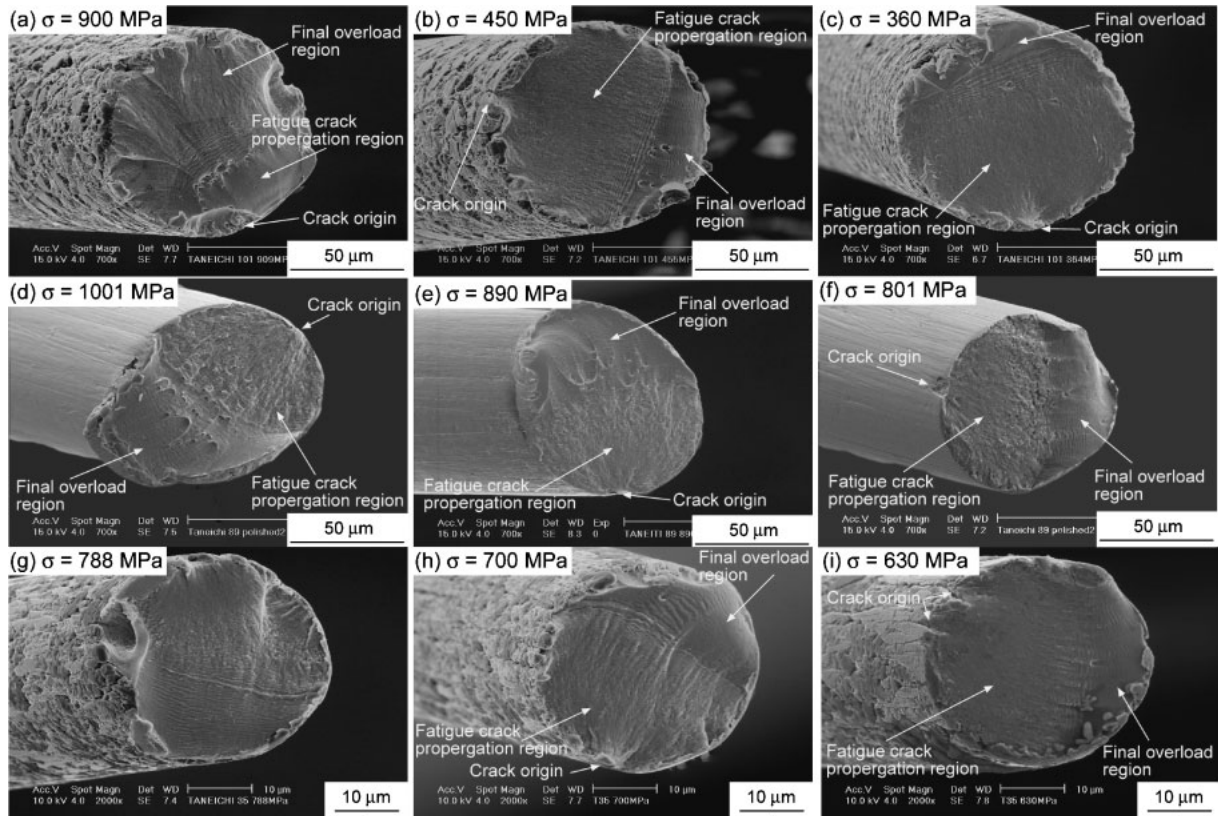


Fig. 3 SEM images of fracture surfaces of  $\beta$ -type alloy wires after fatigue testing in 1 mass% lactic acid solution. (a), (b) and (c): Ti-14Mo-3Nb-1.5Zr  $\phi = 100 \mu\text{m}$  (d), (e) and (f): Ti-14Mo-3Nb-1.5Zr  $\phi = 89 \mu\text{m}$  (g), (h) and (i): Ti-14Mo-3Nb-1.5Zr  $\phi = 35 \mu\text{m}$

before fatigue testing, surface defects are observed on the titanium wires with as-drawn surfaces. The cracks probably originate from the surface defects formed during the cold drawing process of the wire and then propagated through the wire.<sup>10)</sup> The decrease in the cross-sectional area of the wire leads to the final overload failure. The fatigue properties of the surface-polished titanium wires might have improved because surface polishing could cause a decrease in the number and size of surface defects.

Figure 4 shows fatigue curves of the  $\alpha$ -type Ti-10Zr alloy wire and  $\alpha$ -type CP titanium wire in 1 mass% lactic acid solution. No clear fatigue limit is observed for the  $\alpha$ -type titanium wires, and their fatigue strength gradually decreases with decreasing maximum bending stress. In this study, the fatigue limit of the  $\alpha$ -type titanium wires is defined as the fatigue strength at which no failure is observed up to  $10^7$  cycles. The Ti-10Zr alloy wire and CP titanium wire did not fail up to  $10^7$  cycles at maximum bending stresses of

368 MPa and 275 MPa, respectively, which implies that their fatigue limits are in the ranges of 368–440 MPa and 275–367 MPa, respectively. As shown in Fig. 2, the  $\beta$ -type titanium alloy wires show a clear fatigue limit independent of surface roughness and wire diameter. The difference between crystal structures of the  $\beta$ - and  $\alpha$ -type titanium alloys might be the cause of the difference in shapes of the fatigue curves of these wires in rotating-bending fatigue testing. The crystal structures of  $\alpha$ - and  $\beta$ -type titanium materials are hcp (hexagonal close-packed) and bcc (body-centered cubic), respectively. Other research groups have been also obtained fatigue curves with clear and unclear fatigue limits for  $\beta$ -type Ti-29Nb-13Ta-4.6Zr alloy<sup>11)</sup> and  $\alpha$ -type Ti-5Al-2.5Sn alloy,<sup>12)</sup> respectively. The  $\alpha + \beta$  type titanium alloys such as Ti-6Al-4V and Ti-4.5Al-3V-2Fe-2Mo showed clear fatigue limits.<sup>13)</sup> These studies suggest that the  $\beta$  phase in titanium with higher Peierls potential than  $\alpha$  phase causes the clear fatigue limit.

Figures 5(a)–(c) show the fracture surfaces of the Ti-10Zr alloy wire after fatigue testing at maximum bending stresses of 733 MPa, 550 MPa and 489 MPa, respectively. The crack origin, the fatigue crack propagation region and the final overload region are detected on the fracture surfaces shown in Figs. 5(b) and (c) as well as on the fracture surface of  $\beta$ -type titanium alloy wires shown in Fig. 3. The fracture surface of the  $\alpha$ -type Ti-10Zr alloy wire is considerably rougher than those of the  $\beta$ -type Ti-14Mo-3Nb-1.5Zr alloy wires. The reason for this difference in the surface roughness could not be revealed in this study.

### 3.2 Hardness of wires

Hardness distributions of the cross sections of titanium wires before fatigue testing are shown in Fig. 6. The hardness values of fine wires such as the Ti-14Mo-3Nb-1.5Zr alloy wire with the diameter of 35  $\mu\text{m}$ , the Ti-10Zr alloy wire and the CP titanium wire are higher around the center than in the outer region. On the other hand, the hardness distributions of the Ti-14Mo-3Nb-1.5Zr alloy wires with diameters of 89  $\mu\text{m}$  and 100  $\mu\text{m}$  are uniform; further, the hardness values around the centers of these wires are lower than that around the center of the Ti-14Mo-3Nb-1.5Zr alloy wire with the diameter of 35  $\mu\text{m}$ . The higher hardness of the fine wires may be attributed to work hardening during the cold drawing process. Another possible reason for the high hardness is the solution hardening of oxygen from titanium oxide film used for lubrication during the cold drawing process of the fine wires. However, the higher hardness around the center than in the outer region suggests that the effect of the solution hardening of oxygen on wire hardness is small. The oxide film used for lubrication in the drawing process of the  $\beta$ -type titanium alloy wires was formed by anodic oxidation. It is well known that low process temperature of anodic oxidation as compared to that of air oxidation can cause suppression of incorporation of oxygen in the wire. It was reported that severe drawing of an austenitic stainless steel wire resulted in a higher hardness around the center than in the outer region of the wire;<sup>14)</sup> this result is in good agreement with the results of the hardness distribution of the fine titanium wires in this study, shown in Fig. 6(a).

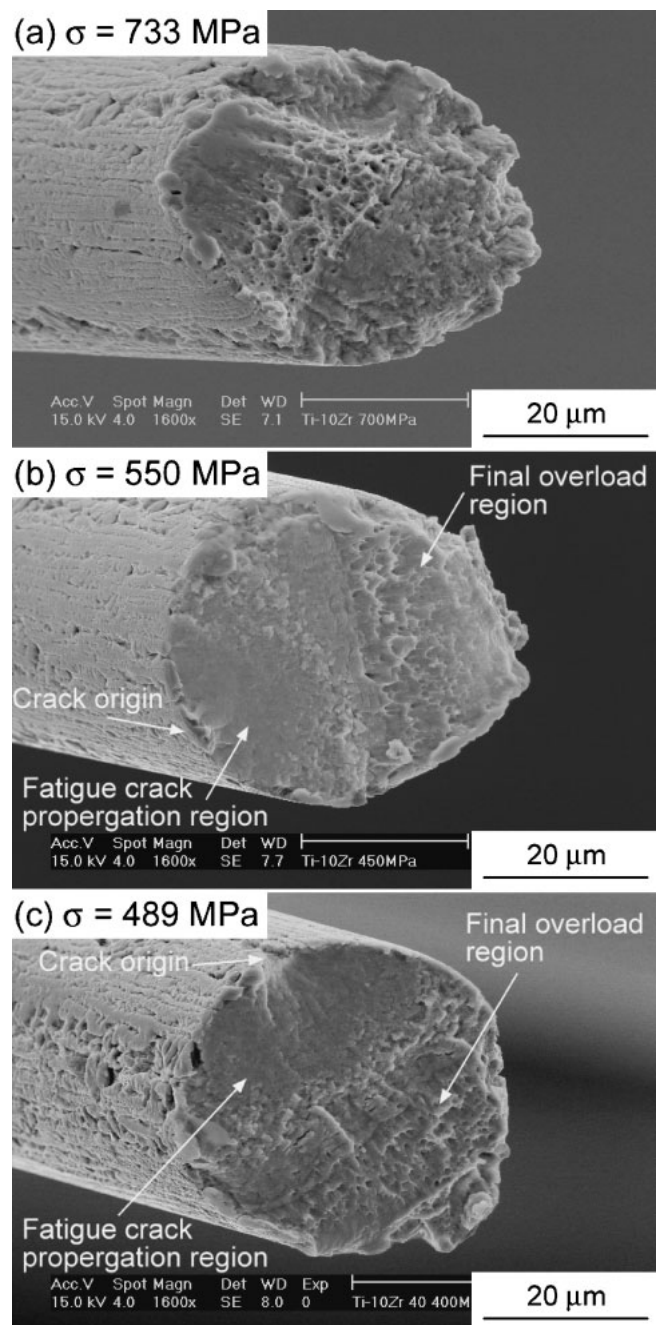


Fig. 5 SEM images of fracture surfaces of  $\alpha$ -type Ti-10Zr alloy wires with a diameter of 40  $\mu\text{m}$  after fatigue testing in 1 mass% lactic acid solution.

### 3.3 Ratio of fatigue limit to tensile strength

Figure 7 summarizes the relationship between the tensile strength ( $\sigma_U$ ) and the fatigue limit ( $\sigma_f$ ) of the titanium wires. It is empirically known that the fatigue strength of the titanium materials in rotating-bending fatigue testing is approximately 40% to 60% of their tensile strength.<sup>15)</sup> In this study, the values of  $\sigma_f/\sigma_U$  for the titanium wires with as-drawn surfaces were less than 0.5, while that for the polished titanium wire was greater than 0.5. As shown in Figs. 3 and 5, the crack origin was observed at the edges of the fracture surfaces. The surface defects that were introduced during the cold drawing process might act as crack origins of the fatigue fracture, and they appear to cause a decrease in the value of  $\sigma_f/\sigma_U$ . Therefore, in order to improve the fatigue properties

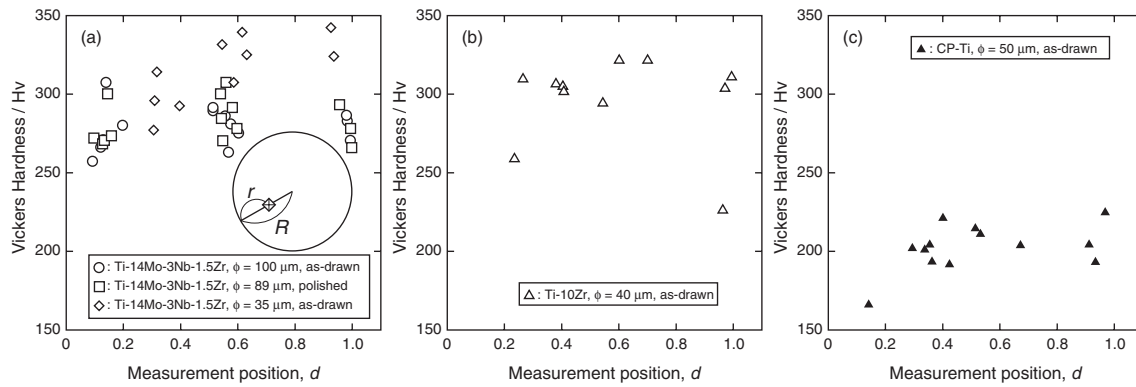


Fig. 6 Hardness distributions of cross sections of (a)  $\beta$ -type titanium wires, (b)  $\alpha$ -type Ti-10Zr alloy wire and (c)  $\alpha$ -type CP titanium wire before fatigue testing. Here,  $d$  is defined as  $r/R$ , where  $r$  and  $R$  are the distances of the measurement position from the outer surface and radius of the wire, respectively.

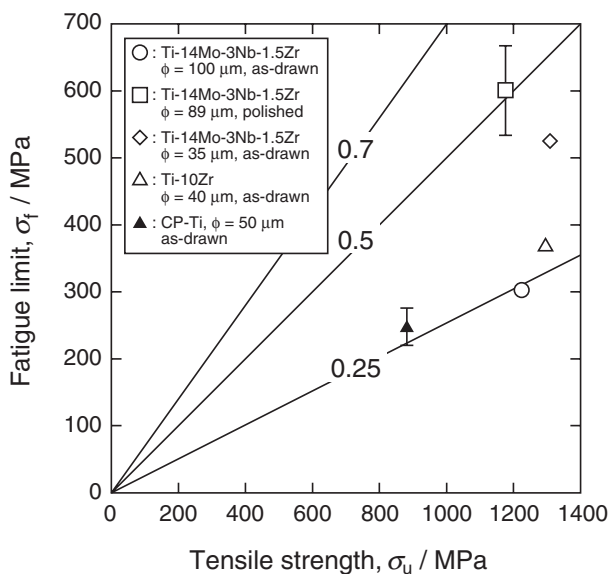


Fig. 7 Relationship between tensile strength and fatigue limit of titanium wires.

of as-drawn titanium wires under biological conditions, it is important to optimize the cold drawing process.

The  $\sigma_f/\sigma_u$  value of the Ti-14Mo-3Nb-1.5Zr alloy wire with the diameter of  $35 \mu\text{m}$  was higher than that with the diameter of  $100 \mu\text{m}$ ; that is, the  $\sigma_f/\sigma_u$  value increased with a decrease in the diameter of the wire. This tendency of the  $\sigma_f/\sigma_u$  value might be attributed to the possibility of presence of the severe defects on the surface of the wire.

### 3.4 Metallic ion elution

Figures 8 and 9 show concentrations of metallic ions eluted from the Ti-14Mo-3Nb-1.5Zr and Ti-10Zr alloy wires, respectively, into the 1 mass% lactic acid solution as functions of the cycle numbers. The arrowheads in these figures indicate that the ion concentration was below the ICP-AES detection limit considered in this study. The concentrations of Nb and Zr ions eluted from the Ti-14Mo-3Nb-1.5Zr alloy wires and Ti and Zr ions eluted from the Ti-10Zr alloy wire were less than  $10^{-2}$  mass ppm. Although the concentration of Ti and Mo ions eluted from the Ti-14Mo-

3Nb-1.5Zr alloy wires increased with an increase in the duration of fatigue testing, the total elution of metallic ions was suppressed to less than  $10^{-1}$  mass ppm. It appears that surface polishing causes a decrease in the elution of Ti and Mo ions for short cycles of fatigue testing of Ti-14Mo-3Nb-1.5Zr alloy wires. Table 2 summarizes the concentrations of metallic ions eluted from the Ti-14Mo-3Nb-1.5Zr and Ti-10Zr alloy wires during the static immersion test in 1 mass% lactic acid solution for 600 ks. The elution of metallic ions in the static immersion test was less than that in fatigue testing. These results suggest that the new surface formed by crack propagation causes the elution of Ti and Mo ions from the titanium wires, though the extent of elution is small.

## 4. Conclusions

Fatigue behaviors of ultra fine wires of  $\beta$ -type Ti-14Mo-3Nb-1.5Zr alloy and  $\alpha$ -type Ti-10Zr alloy and  $\alpha$ -type CP titanium with diameters in the range of  $35\text{--}100 \mu\text{m}$  were investigated by rotating-bending fatigue testing in 1 mass% lactic acid solution maintained at 310 K. The following are the findings of the investigation.

- (1) The  $\beta$ -type Ti-14Mo-3Nb-1.5Zr alloy wires showed a clear fatigue limit independent of the surface roughness and wire diameter. On the other hand, the  $\alpha$ -type Ti-10Zr alloy wire and  $\alpha$ -type CP titanium wire did not show a clear fatigue limit, and their fatigue strengths gradually decreased with decreasing maximum bending stress. The difference in crystal structures of  $\beta$ - and  $\alpha$ -type titanium alloys might be the cause of the difference in shapes of the fatigue curves of these wires in rotating-bending fatigue testing.
- (2) The fracture surface consisted of a fatigue crack propagation region and a final overload region. The crack origin was observed at the edges of the fracture surfaces. Surface defects that were introduced during the cold drawing process might act as crack origins of the fatigue fracture.
- (3) The ratio of the fatigue limit to the tensile strength of the titanium wires with as-drawn surfaces was less than 0.5, while that of the titanium wire with a polished surface was greater than 0.5. Surface polishing could cause a decrease in the number and size of surface

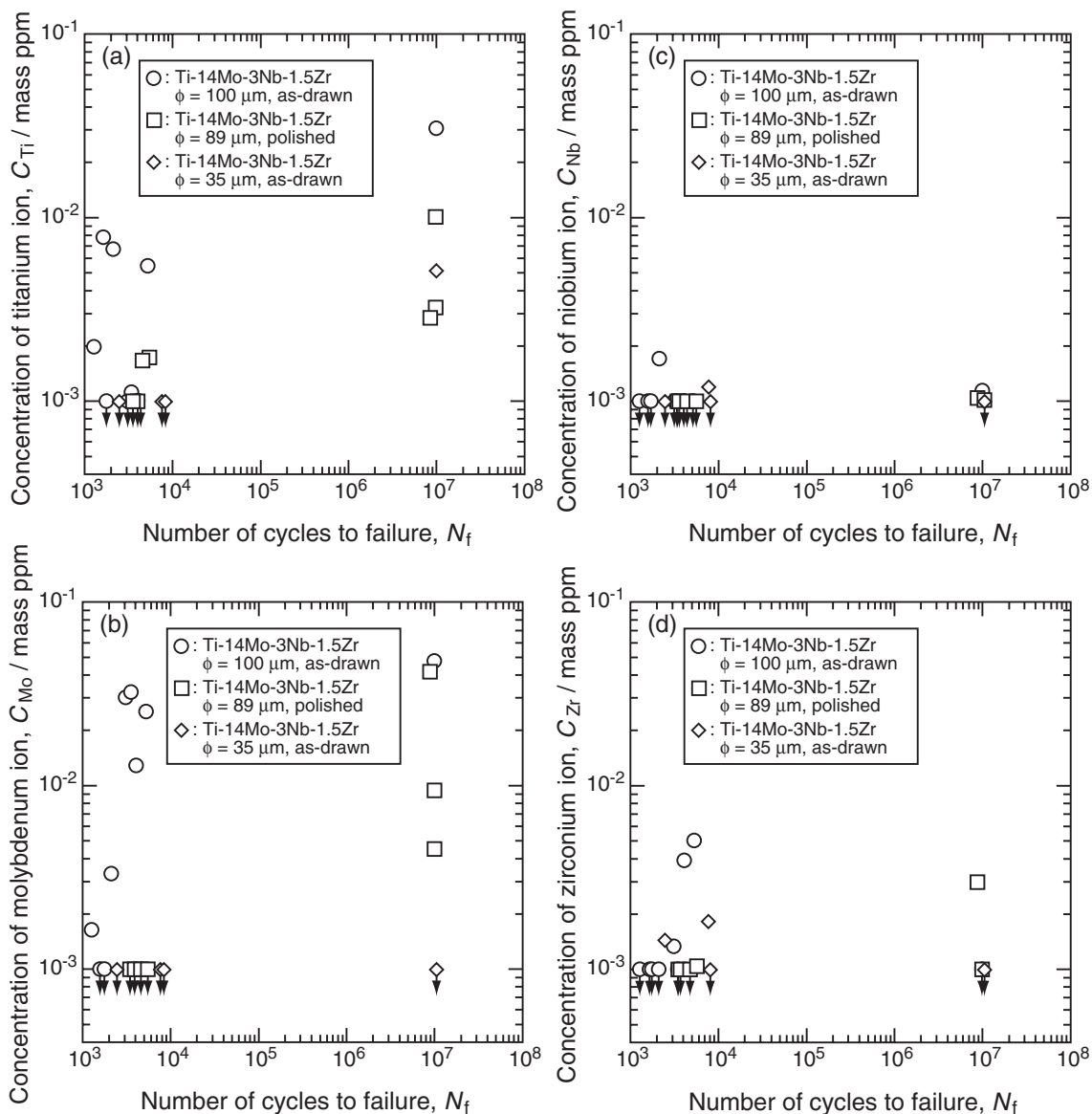


Fig. 8 Changes in concentrations of (a) titanium, (b) molybdenum, (c) niobium and (d) zirconium ions eluted from  $\beta$ -type Ti-14Mo-3Nb-1.5Zr alloy wires during fatigue testing.

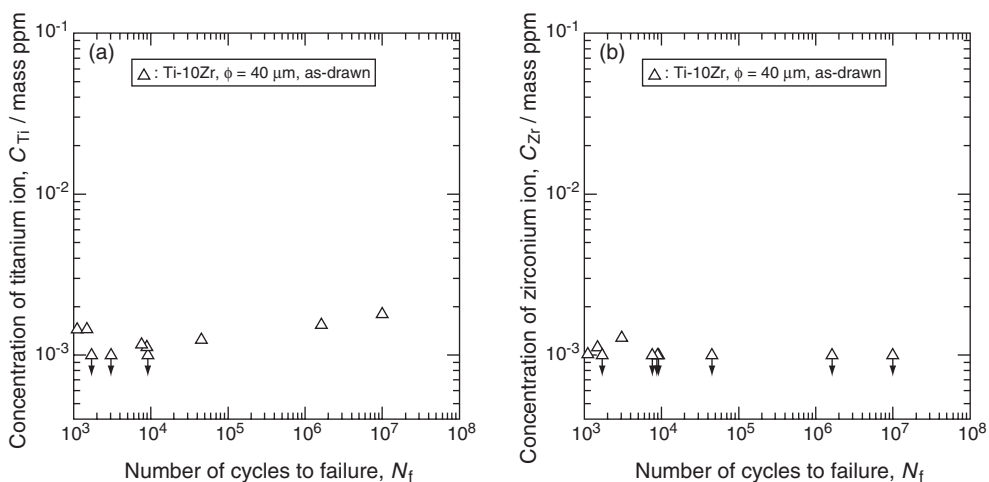


Fig. 9 Changes in concentrations of (a) titanium and (b) zirconium ions eluted from  $\alpha$ -type Ti-10Zr alloy wire during fatigue testing.

Table 2 Concentration of metallic ions (mass ppm) eluted from Ti-14Mo-3Nb-1.5Zr and Ti-10Zr wires during static immersion test in 1 mass% lactic acid solution for 600 ks.

Materials	Diameter ( $\mu\text{m}$ )	Surface	Ti	Mo	Nb	Zr
Ti-14Mo-3Nb-1.5Zr	100	as-drawn	$7 \times 10^{-3}$	$<10^{-3}$	$<10^{-3}$	$<10^{-3}$
Ti-14Mo-3Nb-1.5Zr	89	polished	$<10^{-3}$	$<10^{-3}$	$<10^{-3}$	$<10^{-3}$
Ti-14Mo-3Nb-1.5Zr	35	as-drawn	$3 \times 10^{-3}$	$<10^{-3}$	$<10^{-3}$	$<10^{-3}$
Ti-10Zr	40	as-drawn	$<10^{-3}$	—	—	$<10^{-3}$

defects and might bring about an improvement in the fatigue properties of the titanium wires.

- (4) The metallic ions were suggested to have been eluted from the new surface formed by crack propagation during fatigue testing. However, due to the high corrosion resistance of the titanium wires, their elution into 1 mass% lactic acid solution was suppressed at a very low level.

### Acknowledgements

The authors would like to express their thanks to Hiyama Rare-Metal Industry for supplying the Ti-10Zr alloy wire used in fatigue testing. This work was financially supported by The Light Metal Educational Foundation, Inc., the Special Education and Research Program “Highly-functional Interface Science: Innovation of Biomaterials with Highly Functional Interface to Host and Parasite” by the JSPS and a Grant-in-Aid for Scientific Research from the Ministry of

Education, Culture, Sports, Science and Technology, Japan, under Contract No. 19360324.

### REFERENCES

- 1) A. Scheiner, G. Polando and E. B. Marsolais: IEEE Trans. Biomed. Eng. **41** (1994) 425–431.
- 2) Y. Handa, N. Hoshimiya, Y. Iguchi and T. Oda: IEEE Trans. Biomed. Eng. **36** (1989) 705–710.
- 3) T. Narushima, K. Suzuki, T. Murakami, C. Ouchi and Y. Iguchi: Mater. Trans. **46** (2005) 2083–2088.
- 4) N. Hoshimiya, H. Higa, T. Watanabe, H. Murakami, R. Futami, H. Matsuki, Y. Iguchi, Y. Handa, K. Takahashi, T. Furukawa, Y. Ogasawara and T. Shimotomai: Med. Biolo. Eng. Comp. **34** Supp. 1 Pt.2 (1996) 281–282.
- 5) M. Niinomi, T. Hanawa and T. Narushima: JOM J. Miner. Met. Mater. Soc. **57**[4] (2005) 18–24.
- 6) K. Taneichi, M. Taira, E. Sakedai, T. Narushima, Y. Iguchi and C. Ouchi: ISIJ International **46** (2006) 292–301.
- 7) M. Kato, H. Abe, M. Saka, M. Kurashige, K. Ito and Y. Shindo: *Mechanics of Materials*, (Asakura Publishing, Tokyo, 1988) pp. 69–70.
- 8) T. Nishimura: *Process Technology in Titanium*, (Nikkan Kogyo Shinbun, Tokyo, 1992) p. 9.
- 9) C. R. Brooks and A. Choudhury: *Metallurgical Failure Analysis*, (McGraw-Hill, NY, 1993) p. 232.
- 10) S. Nishijima and K. Kanazawa: Fatigue Fract. Engng. Mater. Struct. **22** (1999) 601–607.
- 11) S. J. Li, M. Niinomi, T. Akahori, T. Kasuga and Y. L. Hao: Biomaterials **25** (2004) 3369–3378.
- 12) Y. Ono, T. Yuri, H. Sumiyoshi, S. Matsuoka and T. Ogata: Cryogenics **44** (2003) 483–489.
- 13) K. Nakajima, K. Terao and T. Miyata: Mat. Sci. Eng. A **243** (1998) 176–181.
- 14) Drawing: from fundamentals to up-to-date techniques, (Corona Publishing, Tokyo, 1990) p. 82.
- 15) *Fatigue Design Handbook*, (Yokendo, Tokyo, 1995) p. 10.